



# Lumbar spine angles and intervertebral disc characteristics with end-range positions in three planes of motion in healthy people using upright MRI



David B. Berry<sup>a</sup>, Alejandra Hernandez<sup>b</sup>, Keenan Onodera<sup>c</sup>, Noah Ingram<sup>b</sup>, Samuel R. Ward<sup>a,c,d</sup>, Sara P. Gombatto<sup>b,\*</sup>

<sup>a</sup> Department of Bioengineering, University of California San Diego, La Jolla, CA, USA

<sup>b</sup> Doctor of Physical Therapy Program, School of Exercise and Nutritional Sciences, San Diego State University, San Diego, CA, USA

<sup>c</sup> Department of Orthopaedic Surgery, University of California San Diego, La Jolla, CA, USA

<sup>d</sup> Department of Radiology, University of California San Diego, La Jolla, CA, USA

## ARTICLE INFO

Article history:  
Accepted 12 April 2019

Keywords:  
Lumbar spine  
Posture  
Kinematics  
Upright MRI  
Intervertebral disc

## ABSTRACT

Understanding changes in lumbar spine (LS) angles and intervertebral disc (IVD) behavior in end-range positions in healthy subjects can provide a basis for developing more specific LS models and comparing people with spine pathology. The purposes of this study are to quantify 3D LS angles and changes in IVD characteristics with end-range positions in 3 planes of motion using upright MRI in healthy people, and to determine which intervertebral segments contribute most in each plane of movement. Thirteen people (average age = 24.4 years, range 18–51 years; 9 females; BMI =  $22.4 \pm 1.8 \text{ kg/m}^2$ ) with no history of low back pain were scanned in an upright MRI in standing, sitting flexion, sitting axial rotation (left, right), prone on elbows, prone extension, and standing lateral bending (left, right). Global and local intervertebral LS angles were measured. Anterior-posterior length of the IVD and location of the nucleus pulposus was measured. For the sagittal plane, lower LS segments contribute most to change in position, and the location of the nucleus pulposus migrated from a more posterior position in sitting flexion to a more anterior position in end-range extension. For lateral bending, the upper LS contributes most to end-range positions. Small degrees of intervertebral rotation ( $1\text{--}2^\circ$ ) across all levels were observed for axial plane positions. There were no systematic changes in IVD characteristics for axial or coronal plane positions.

© 2019 Elsevier Ltd. All rights reserved.

## 1. Introduction

Low back pain (LBP) is one of the most common musculoskeletal complaints, affecting 70%–85% of the population in their lifetime (Andersson, 1999). Understanding the alignment and movement of the lumbar spine (LS) in healthy people is important to identify postural and kinematic changes associated with aging, injury, and pathology. Additionally, estimates of both normal and abnormal LS alignment and movement are necessary to inform musculoskeletal models of the spine. Several investigators have examined lumbar intervertebral biomechanics *ex vivo* at a single motion segment (Gunzburg et al., 1991; Kettler et al., 2004;

Panjabi et al., 1983; Panjabi and White III, 1990). However, it is difficult to apply these findings to the complex loading conditions in the entire LS over the full range of normal human motion. Therefore, there is interest in investigating whole LS biomechanics *in vivo*.

Noninvasive imaging has been used to measure 3D LS posture and movement *in vivo*. The most common modalities include optical motion capture (Gombatto et al., 2007; Scholtes et al., 2009), dual-fluoroscopy (Li et al., 2009; Wang et al., 2008; Wu et al., 2014), and magnetic resonance imaging (MRI) (Madsen et al., 2008; Simonetti and Masala, 2003). The main advantage to optical motion capture is high temporal resolution, however, measurements are limited to surface markers on the skin and may not directly reflect underlying bony alignment or movement (Li et al., 2009; MacWilliams et al., 2014; Wang et al., 2008; Yang et al., 2008). Dual-fluoroscopy affords high-temporal resolution and has been used to measure motion of the spine in end-range positions

\* Corresponding author at: Doctor of Physical Therapy Program, School of Exercise and Nutritional Sciences, San Diego State University, 5500 Campanile Drive, San Diego, CA 92182-7251, USA.

E-mail address: [sgombatto@sdsu.edu](mailto:sgombatto@sdsu.edu) (S.P. Gombatto).

in 3D. However, this method utilizes ionizing radiation, cannot simultaneously measure all levels of the LS due to the limited field of view, and requires volumetric registration of the vertebrae – measured with either CT or MRI – to 2D images, which is labor intensive and computationally complex. Further, neither optical motion capture nor dual-fluoroscopy allow for simultaneous capture of bony and soft tissue structures. Lumbar intervertebral disc (IVD) health has been implicated in the development and persistence of LBP and can affect lumbar posture (Berry et al., 2017; Keorochana et al., 2011; Lao et al., 2015). Therefore, IVD changes with physiologically relevant positions are also important to consider.

MRI provides a non-invasive approach to measure both changes in posture and IVD characteristics in the entire LS without ionizing radiation. The main limitation of traditional MRI is subjects are supine, which does not account for physiologic loading associated with weight bearing. Some investigators have attempted to replicate loading associated with weight bearing in traditional scanners (Choi et al., 2009; Saifuddin et al., 2003; Willén et al., 1997). However, advances in upright MRI technology provide the ability to image the bony and soft tissue structures simultaneously in functional, weight-bearing positions. It has been used to measure sagittal LS posture under different loading conditions and positions in highly active populations (Berry et al., 2017; Rodriguez-Soto et al., 2016a; Rodriguez-Soto et al., 2016b; Rodriguez-Soto et al., 2013), children (Neuschwander et al., 2010; Shymon et al., 2014a,b) and adults with and without LBP (Keorochana et al., 2011; Kong et al., 2009; Li et al., 2009; Nguyen et al., 2016; Tarantino et al., 2013). Investigators have also reported changes in IVD morphometry between the traditional supine and weight-bearing positions such as sitting and standing (Gilbert et al., 2010; Nazari et al., 2012, 2015; Tarantino et al., 2013), and limited ranges of flexion and extension (Alexander et al., 2007; Alyas et al., 2010; Hayashi et al., 2015; Hedberg et al., 2013; Lee et al., 2009; Zou et al., 2009). However, to our knowledge, changes in LS posture and IVD characteristics, in end-range sagittal, coronal, and axial positions in a healthy population is unknown. Therefore, the purposes of the current study are: (1) to quantify 3D LS posture and IVD characteristics with end-range positions in 3 planes of movement, and (2) to determine which intervertebral segments contribute most in each plane of movement in healthy people with upright MRI.

## 2. Methods

### 2.1. Participants

The San Diego State University Institutional Review Board approved the study, and all volunteers provided oral and written informed consent prior to participation. Each participant verbally confirmed no lifetime history of LBP or LS pathology during screening and on the day of testing.

### 2.2. Imaging

Subjects were scanned using an upright 0.6T MRI scanner (Fonar Corporation, Melville, NY) and a quad-planar coil. An elastic band was used to hold the coil against the LS between the L1–S1 levels; the band was secured to hold the coil in place while allowing the subject to maintain a natural position. A three-plane localizer and sagittal T2-weighted MRI were acquired as previously reported (Berry et al., 2017).

Subjects were scanned in the following positions: standing, standing left lateral bending, standing right lateral bending, sitting left trunk rotation, sitting right trunk rotation, sitting forward flex-

ion, prone on elbows (POE), and prone extension (PEExt) with arms fully extended (Fig. 1). Position order was block randomized (blocks: standing, sitting, and prone) to control for order effects. Subjects were instructed on how to assume each position, and were asked to move as far as they could in each direction and hold each position for the duration of the MRI acquisition. Each position is depicted and described, along with the explicit verbal instructions given to each subject in Appendix A.

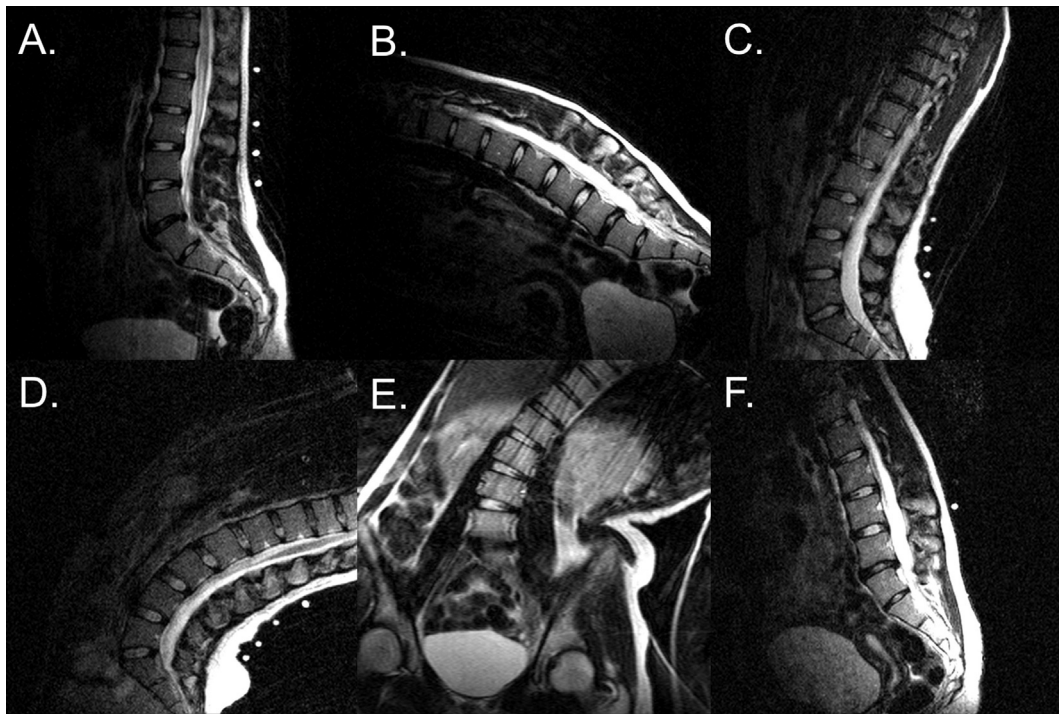
### 2.3. LS angle measurements

Global LS and intervertebral angle measurements were generated from upright MRI images in each position, using a previously validated algorithm (available at [muscle.ucsd.edu/downloads](http://muscle.ucsd.edu/downloads)) (Berry et al., 2015). Briefly, digital seed points were manually placed on the corners of the vertebral body and on the posterior elements of each vertebra by a single rater using OsiriX (Rosset et al., 2004). The locations of the seed points were checked and verified by a second rater before being imported into MatLab (MathWorks Inc., Natick, MA) and used to define an endplate-based joint coordinate system applied to each vertebra (L1–S1). This approach was selected to directly reflect position of the motion segment, and because there is less measurement error associated with an endplate-based approach when compared to a vertebral body-based method (Berry et al., 2015). Error (RMS) using this technique is 0.95° for sagittal, 1.09° for axial, and 1.66° for coronal plane angle measurements (Berry et al., 2015). Inter-rater agreement for this technique, using images from the prior validation study, indicate excellent agreement (ICC > 0.9) between raters (unpublished data).

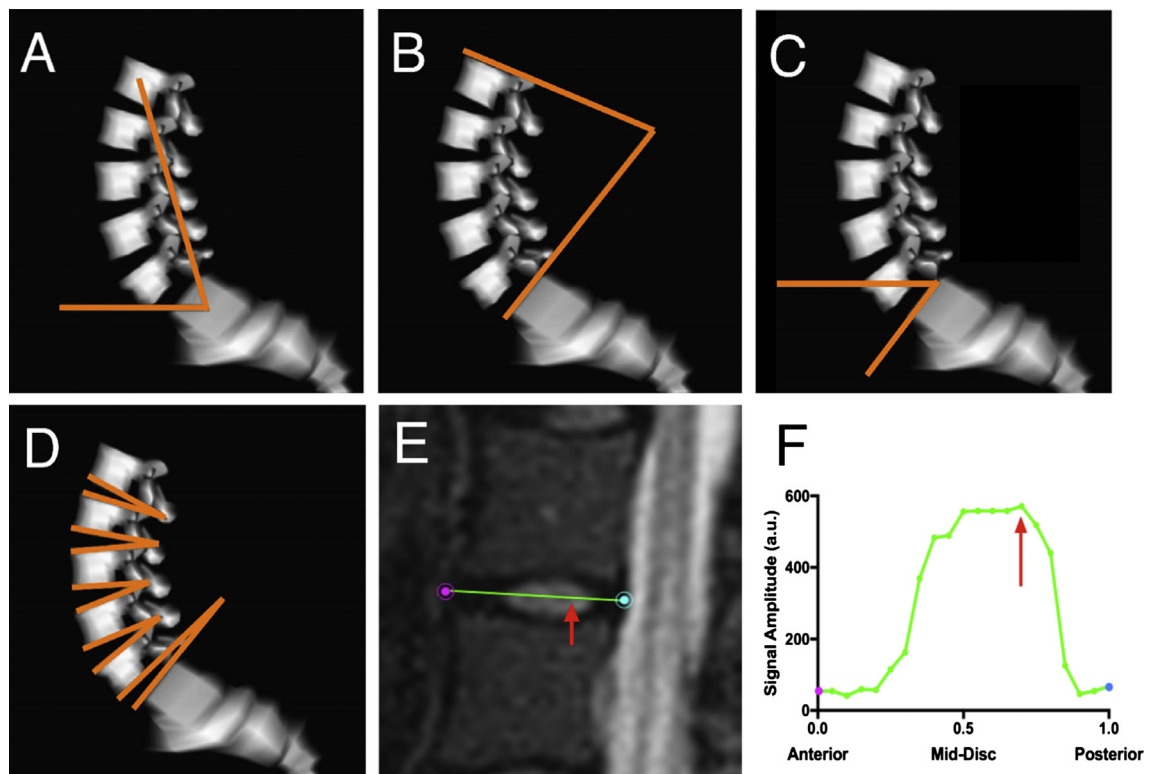
Global measurements of LS posture and local intervertebral angles were calculated for all positions (Fig. 2A–D). Global measurements included LS angle with respect to the horizontal (AwrtH), sacral slope, and Cobb angle. The AwrtH indicates the degree of inclination of the entire LS in the sagittal plane, and is defined as the angle between a line connecting the geometric centroids of L1 and S1, and a line perpendicular to gravity, directed anteriorly. Sacral slope describes the orientation of the sacrum to provide an estimate of pelvic inclination, and is defined as the angle between the superior endplate of S1 and the horizontal. For horizontal postures (POE and PEExt) the reference frame for orientation of AwrtH and sacral slope was rotated 90°. The Cobb angle is used to measure the curvature of the spine and is defined as the angle between the superior endplate of L1 to the superior endplate of S1 (Cobb, 1948). Local intervertebral angles were measured between the superior and inferior endplates of adjacent vertebrae to characterize the 3D orientation of adjacent vertebrae throughout the LS in each position. A positive value is indicative of lumbar lordosis (extension) in the sagittal plane, right lateral bending in the coronal plane, and left rotation in the axial plane.

### 2.4. IVD measurements

IVD height was measured as the anterior and posterior Euclidean distance between planes fit to the endplates of each vertebra. Anterior-posterior (A/P) length of the IVD and location of the nucleus pulposus (NP) was measured for all positions using custom software developed in MatLab. The anterior and posterior margins of each IVD were manually identified, and the distance between them was calculated to determine the A/P length. The profile of signal intensity between these two points was extracted and the location of maximum signal intensity within the NP was determined, to track A/P NP location (Brault et al., 1997; Edmondston et al., 2000) (Fig. 2E–F).



**Fig. 1.** Representative MRI images of a participant in (A) Standing (B) Sitting flexion (C) Prone on elbows (*image rotated 90°*) (D) Prone extension (*image rotated 90°*) (E) Standing left lateral bending (F) Sitting left rotation positions.



**Fig. 2.** Schematics depicting global and local lumbar spine angles and a representative measurement of IVD characteristics from MRI images. Measurements included (A) Lumbar angle with respect to the horizontal to assess lumbar spine inclination. (B) Cobb angle to measure lumbar lordosis. (C) Sacral slope to assess inclination of the pelvis. (D) Intervertebral angles to provide a measurement of local lumbar alignment. (E) Anterior-posterior disc length and nucleus pulposus position. A point on the anterior (pink) and posterior (blue) margins of the intervertebral disc are identified. (F) The signal intensity profile of the line between the two points is extracted (green), and the local maximum of the signal intensity is identified (red arrow). (For interpretation of the references to colour in this figure legend, the reader is referred to the web version of this article.)

### 2.5. Statistical analyses

Positions were grouped based on the primary plane of movement. Sagittal plane positions included sitting forward flexion, POE and PExt. Axial plane positions included sitting left and right rotation. Coronal plane positions included standing left and right lateral bending. The standing position was used as a baseline position for all position groups.

Global measurements (AwrtH, sacral angle, and Cobb angle) were compared between positions using one-way repeated measures analysis of variance (ANOVA) tests with post hoc Sidak tests to identify differences between positions. Intervertebral angles, IVD A/P length, and NP location were analyzed using two-way repeated measures ANOVA with post hoc Sidak tests to identify differences between positions and intervertebral levels. Separate tests were conducted for each group of positions (sagittal, coronal, axial). Additionally, within each position group, separate tests were conducted for each plane of motion for intervertebral angles. The threshold for significance ( $\alpha$ ) was set to 0.05 for all analyses. Analyses were conducted using IBM SPSS Statistics 20.0 (IBM, Armonk, NY). All data are reported as mean  $\pm$  standard error.

### 3. Results

Image data sets were obtained from 13 volunteers (average age = 24.4 years, range 18–51 years; 9 females; height =  $1.6 \pm 0.1$  m, weight =  $64.3 \pm 1.2$  kg, BMI =  $22.4 \pm 1.8$  kg/m<sup>2</sup>). Data from POE and PExt positions were excluded for one subject due to motion artifact. Lateral bending data were excluded for two subjects due to motion artifact. Spinal abnormalities were not observed in any participant. Global LS angle measurements for all positions are reported in Table 1. Intervertebral angle measurements for all positions are reported in Table 2. IVD height measurements for all positions are reported in Supplement 1. De-identified subject data is available upon reasonable request.

There were significant differences in all global LS measurements among sagittal plane positions ( $p < .001$ ; Fig. 3A–C). LS AwrtH increased from sitting forward flexion ( $29.2^\circ \pm 13.4^\circ$ ) to PExt ( $119.3^\circ \pm 8.3^\circ$ ), however there was no significant difference between standing and POE positions ( $p = .989$ ). There was a significant difference in sagittal Cobb angle ( $p < .01$ ) and sacral slope ( $p < .01$ ) between all sagittal plane positions. The sagittal Cobb angle increased from sitting flexion ( $0.1^\circ \pm 1.8^\circ$ ) to PExt ( $76.8^\circ \pm 2.0^\circ$ ), while the sacral slope was greatest in sitting flexion ( $69.2^\circ \pm 10.8^\circ$ ) and smallest in PExt ( $23.1^\circ \pm 7.4^\circ$ ). There were small, significant differences in coronal Cobb angles between sagittal positions ( $p < .05$ ; Table 1). For sagittal intervertebral angles, there was a significant effect of level ( $p < .001$ ), position ( $p < .001$ ), and an interaction of level and position ( $p < .001$ ). With end-range flexion in sitting, all segments were in a more flexed position compared to standing and prone positions; on average L1–L5 displayed slight flexion ( $0.8$ – $1.3^\circ$ ), and L5–S1 maintained  $3.0^\circ$  of extension

(Fig. 4A). A significant increase in intervertebral extension was observed at the L1–L2, L2–L3 and L5–S1 levels when subjects were POE compared to the standing position ( $p < .05$ ). Compared to POE, there was a significant increase in intervertebral extension with PExt in all segments ( $p < .01$ ) except L2–L3 ( $p = .381$ ). For coronal intervertebral angles, there was no effect of position ( $p = .458$ ) or level ( $p = .151$ ); the interaction of position and level approached significance ( $p = .080$ ). For axial intervertebral angles, there was no effect of position ( $p = .335$ ), level ( $p = .882$ ), or interaction effect of position and level ( $p = .363$ ).

There was a significant difference in coronal Cobb angle among coronal plane positions ( $p < .001$ ). Subjects had a larger coronal Cobb angle when bending to the left ( $-25.2^\circ \pm 8.3^\circ$ ) and to the right ( $23.5^\circ \pm 12.9^\circ$ ) compared to standing ( $2.1^\circ \pm 1.4^\circ$ ;  $p < .001$ ; Fig. 5). There were no significant differences in sagittal Cobb angle ( $p = .127$ ), sacral slope ( $p = .145$ ), or LS AwrtH ( $p = .934$ ) among coronal plane positions. For coronal intervertebral angles, there was a significant effect of position ( $p < .001$ ) and interaction effect of position and level ( $p < .001$ ), but no significant effect of level ( $p = .634$ ). Significant differences between positions were found at every level between standing and each side bending position ( $p < .01$ ; Fig. 4B), with the exception of L5–S1 between standing and left lateral bending ( $p = .999$ ). For sagittal intervertebral angles, there was a significant effect of position ( $p < .05$ ), level ( $p < .001$ ), and interaction effect of position and level ( $p < .01$ ). Post hoc tests indicated a significant difference with greater extension at L5–S1 in standing ( $11.1^\circ \pm 4.4^\circ$ ) than with left bending ( $3.2^\circ \pm 2.5^\circ$ ;  $p < .01$ ) and right bending ( $3.9^\circ \pm 2.6^\circ$ ;  $p < .001$ ), which were not different from one another ( $p = .866$ ; Table 2). For axial intervertebral angles, there was no effect of position ( $p = .327$ ) or interaction of position and level ( $p = .109$ ), but the effect of level approached statistical significance ( $p = .062$ ) (see Supplement data).

For axial plane positions, there was a significant difference among positions for sagittal Cobb ( $p < .001$ ), sacral slope ( $p < .001$ ), LS AwrtH ( $p = .018$ ), and coronal Cobb angle ( $p = .015$ ). Sitting rotation resulted in a significant decrease ( $p < .001$ ) in sagittal Cobb angle ( $\sim 30^\circ$ ) and sacral slope ( $\sim 17^\circ$ ) relative to standing. Differences between coronal Cobb angle with sitting left rotation ( $8.2^\circ \pm 11.7^\circ$ ) and sitting right rotation ( $-2.1^\circ \pm 8.5^\circ$ ) approached significance ( $p = .069$ ). For axial intervertebral angles, there was a significant effect of position ( $p < .001$ ) and level ( $p < .05$ ), but no significant interaction of position and level ( $p = .235$ ). Axial intervertebral angles were generally less than  $2^\circ$  different from standing alignment with either direction of sitting rotation (Fig. 4C). For sagittal intervertebral angles with axial plane positions, there was a significant effect of position ( $p < .001$ ), level ( $p < .001$ ), and an interaction of position and level ( $p < .001$ ). Less extension was observed between standing and both sitting positions from L3–L4 to L5–S1 ( $\sim 6$ – $10^\circ$ ;  $p < .001$ ) and between the standing and sitting left rotation positions at L2–L3 ( $3.4^\circ$ ;  $p < .05$ ). For coronal intervertebral angles, there was a significant effect of position ( $p < .05$ ) and interaction of position and level ( $p = .029$ ), but no effect of level

**Table 1**  
Global lumbar spine measures (in degrees) for all positions. Data reported as mean (standard error).

Position	Sagittal Cobb	Coronal Cobb	Lumbar angle w.r.t. horizontal	Sacral slope
Standing	51.1(2.6)	2.1(1.4)	83.3(1.2)	44.5(2.1)
Sitting flexion	0.1(1.8)	1.9(1.1)	29.2(3.7)	69.2(3.0)
Prone on elbows	63.2(2.0)	-2.5(1.2)	81.2(1.2)	36.2(1.6)
Prone extension	76.8(2.0)	-1.2(2.9)	119.2(2.4)	23.1(2.1)
Standing left bend	45.8(3.9)	-25.2(2.5)	81.8(1.8)	42.7(2.4)
Standing right bend	44.5(3.2)	22.6(4.1)	82.4(1.7)	41.7(2.3)
Sitting left axial rotation	20.9(3.1)	8.2(3.2)	79.9(1.6)	27.5(2.7)
Sitting right axial rotation	21.8(3.1)	-2.1(2.4)	79.0(1.9)	27.8(2.8)

**Table 2**

Local intervertebral angles (in degrees) in all cardinal planes for all positions at all levels. **Bold** indicates intervertebral angles for the primary plane of motion. Data reported as mean (standard error).

	Position	L1-L2	L2-L3	L3-L4	L4-L5	L5-S1
Sagittal	Standing	1.7(0.4)	5.0(0.7)	8.7(0.7)	12.4(1.0)	11.1(1.2)
	<b>Sitting flexion</b>	<b>-1.1(0.6)</b>	<b>-1.3(0.4)</b>	<b>-1.1(0.5)</b>	<b>-0.8(0.7)</b>	<b>3.0(0.8)</b>
	<b>Prone on elbows</b>	<b>6.1(0.8)</b>	<b>7.2(0.6)</b>	<b>8.5(0.5)</b>	<b>11.9(1.2)</b>	<b>14.4(1.1)</b>
	<b>Prone extension</b>	<b>8.7(0.8)</b>	<b>8.7(1.1)</b>	<b>11.1(0.8)</b>	<b>15.4(1.1)</b>	<b>18.1(1.6)</b>
	Standing left bend	3.2(0.8)	6.0(0.2)	8.1(0.5)	10.5(0.9)	8.4(1.4)
	Standing right bend	3.3(1.0)	5.6(0.5)	8.6(0.7)	10.1(0.8)	7.8(1.6)
	Sitting left axial rotation	1.7(0.6)	1.6(0.8)	2.3(0.8)	1.9(0.9)	3.2(0.7)
	Sitting right axial rotation	1.6(0.7)	2.5(0.9)	2.3(0.7)	1.7(0.8)	3.9(0.7)
	Coronal	Standing	0.6(0.9)	0.0(0.6)	-1.1(0.7)	1.3(0.8)
Sitting flexion		0.5(0.7)	0.3(1.2)	1.4(0.8)	0.2(0.9)	1.3(1.1)
Prone on elbows		-0.3(0.7)	1.7(1.1)	-0.9(1.2)	0.6(0.7)	0.0(0.7)
Prone extension		1.3(1.1)	0.5(1.6)	-1.1(0.7)	-0.5(1.4)	1.5(1.5)
<b>Standing left bend</b>		<b>-7.5(2.1)</b>	<b>-5.1(1.1)</b>	<b>-4.8(1.0)</b>	<b>-4.0(0.9)</b>	<b>-1.2(1.4)</b>
<b>Standing right bend</b>		<b>9.9(1.9)</b>	<b>8.7(1.6)</b>	<b>6.8(1.8)</b>	<b>6.0(1.2)</b>	<b>3.1(1.6)</b>
Sitting left axial rotation		1.1(1.2)	3.4(1.2)	3.6(1.2)	1.4(0.9)	4.1(1.7)
Sitting right axial rotation		-1.2(1.5)	-2.2(1.2)	-0.3(0.8)	-0.4(1.0)	0.4(1.3)
Axial		Standing	0.6(0.5)	0.2(0.5)	-0.2(0.3)	0.1(0.3)
	Sitting flexion	0.3(0.5)	-0.6(0.6)	0.3(0.3)	0.5(0.5)	0.7(0.5)
	Prone on elbows	0.3(0.2)	0.0(0.2)	0.6(0.3)	-0.3(0.4)	0.3(0.4)
	Prone extension	-0.7(0.9)	0.1(0.8)	-0.1(0.3)	0.1(0.5)	-0.2(0.7)
	Standing left bend	1.2(0.9)	-2.6(1.1)	0.3(1.1)	-0.8(1.2)	0.9(0.9)
	Standing right bend	-1.1(1.2)	0.3(1.2)	0.3(0.8)	0.4(1.2)	1.0(0.4)
	<b>Sitting left axial rotation</b>	<b>0.7(0.6)</b>	<b>-0.6(0.5)</b>	<b>0.6(0.6)</b>	<b>1.3(0.9)</b>	<b>0.6(0.8)</b>
	<b>Sitting right axial rotation</b>	<b>-0.6(0.8)</b>	<b>-2.8(0.7)</b>	<b>-0.2(0.8)</b>	<b>-0.6(0.9)</b>	<b>-0.1(0.5)</b>

( $p = .698$ ). More right lateral bending was observed at L3-L4 with sitting left rotation ( $3.6^\circ \pm 4.3^\circ$ ) than standing ( $-1.1^\circ \pm 2.6^\circ$ ;  $p < .05$ ).

The effect of position on IVD height, A/P IVD length, and A/P NP location are reported in Supplement 1.

#### 4. Discussion

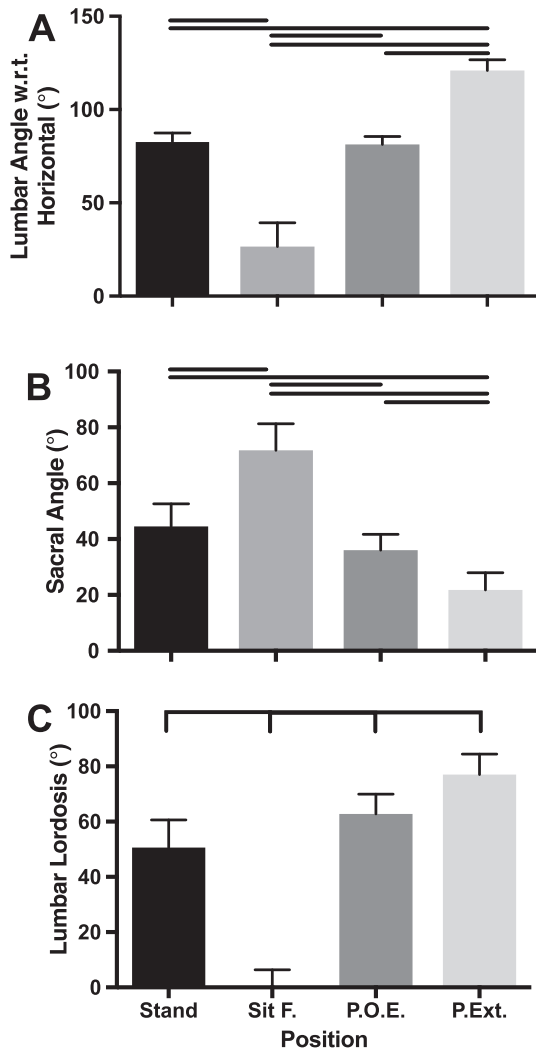
In this study, we evaluated global and local LS angles and IVD characteristics with end-range positions along the cardinal planes of motion in 13 healthy subjects with no history of LBP. Position-dependent changes in global LS angles were found primarily along the main axis of motion and for some out-of-plane measures. For sagittal plane positions, greater differences were observed in lower than upper LS segments; for lateral bending, greater differences in coronal plane angles were observed in the upper LS segments. With sitting rotation, small degrees of rotation were found across intervertebral segments. The IVD length was smaller in end-range sagittal positions, and the NP peak signal intensity changed from a more posterior position in sitting flexion to a more anterior position in end-range extension. This study demonstrates the advantages of using upright MRI to investigate the response of both bony and soft tissue structures of the LS to position changes, and uses software to measure LS angles in 3D that has been validated and is free to use (Berry et al., 2015), which allows for similar studies to be repeated in other cohorts.

The findings of this study add to the body of knowledge from previous studies investigating LS alignment using different techniques. Reported measures of global and local LS angles in the standing and sitting positions are within 2–9° degrees of previous studies using upright MRI (Berry et al., 2017; Karadimas et al., 2006; Rodriguez-Soto et al., 2016a; Rodriguez-Soto et al., 2016b; Rodriguez-Soto et al., 2013). Sagittal plane mobility (from flexion to extension) in the current study is greater than that reported in prior studies of sagittal plane positions using upright MRI, because the prior studies evaluated only early to mid-range sagittal positions (Berry et al., 2017; Keorochana et al., 2011; Kong et al., 2009; Lao et al., 2015). However, overall extension mobility and that less mobility was observed in upper segments than lower

lumbar segments is similar to a study by Kulig et al., who evaluated a similar PExt position (Kulig et al., 2007). Distribution of sagittal plane mobility in the current study is also similar to findings with end-range extension in standing by Pearcy et al., such that less sagittal mobility was observed in upper lumbar segments than lower lumbar segments (Pearcy et al., 1984). These findings differ from other studies that reported sagittal plane motion is greater in upper than lower segments in subjects without LBP who were substantially older than subjects in the current sample (Li et al., 2009; Passias et al., 2011), and greater in central lumbar segments (L2-L4) in people with LBP in early to mid-ranges of motion (Keorochana et al., 2011; Lao et al., 2015). The conflicting evidence suggests that distribution of sagittal plane mobility is different depending on age, range of movement, and LBP status. These factors will need to be considered when modeling lumbar spine mobility.

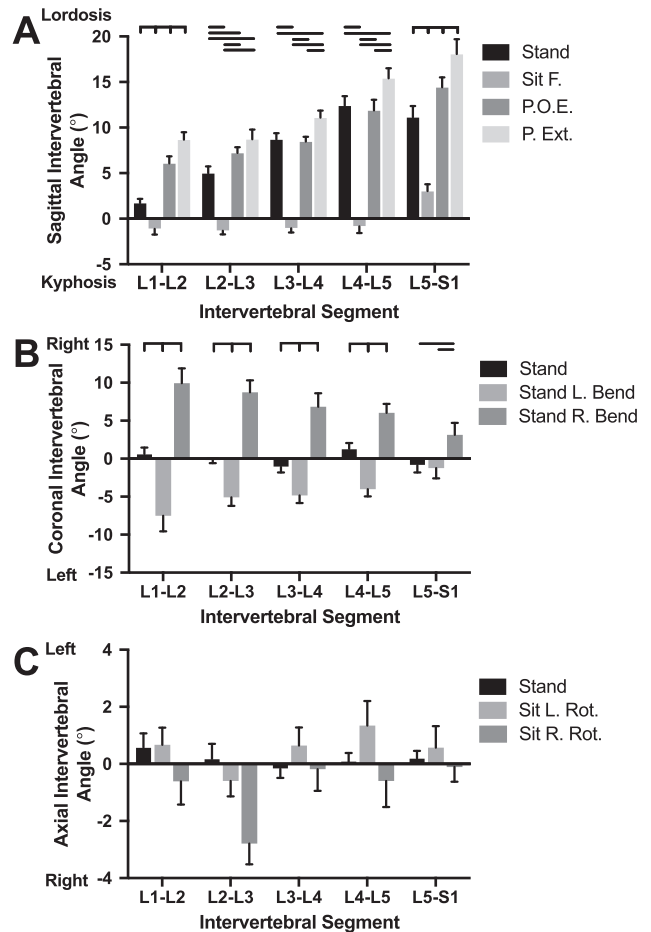
A limited number of investigators have evaluated intersegmental motion during trunk rotation in small samples of healthy subjects ( $n = 8-10$ ). Previous studies reported similar degrees of total intersegmental rotation across segments (2–3°), during maximal trunk rotation in supine unloaded and standing loaded positions (Fujii et al., 2007; Li et al., 2009; Pearcy and Tibrewal, 1984). We found average intervertebral rotation measures ranged from 0.2 to 2.8° in each direction and no significant difference across levels. These data suggest that lumbar rotation kinematics are generally consistent across studies, but the slight difference in magnitude of rotation across studies may be related to the position, or physical constraints limiting rotation in the MRI. Overall, these low measures of intersegmental rotation across studies are likely associated with facet joint orientation in lumbar vertebrae.

There have also been a limited number of investigations to evaluate intersegmental motion with lateral bending movements in healthy subjects. We found greater coronal plane intervertebral mobility in the upper than lower LS, similar to Pearcy et al who also evaluated lateral bending while standing (Pearcy and Tibrewal, 1984). However, these findings are different from Fazey et al., who reported 5–7° at each segment, but no difference across segments with passive lateral bending using supine MRI (Fazey et al., 2010). The differences across studies are likely due

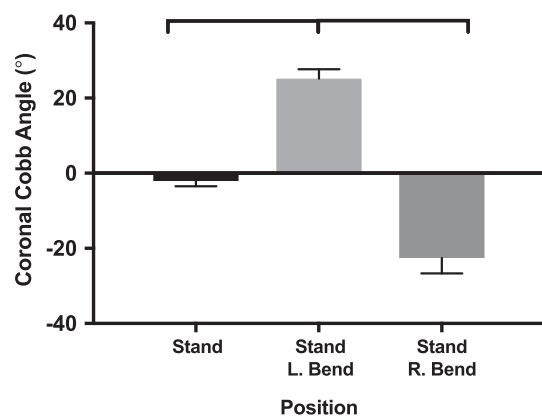


**Fig. 3.** Global lumbar spine angles including lumbar angle with respect to the horizontal (A), sacral slope (B), and lumbar lordosis (C, sagittal Cobb) for sagittal positions (standing, sitting flexion, prone on elbows, prone extension). Statistically significant difference between measurements ( $p < .05$ ) indicated by line. Sit F. = Sitting forward flexion. P.O.E. = Prone on elbows. P. Ext. = Prone extension with elbows extended.

to differences in loaded vs. unloaded positions and passive vs. active movements. Other studies have been conducted to evaluate trunk lateral bending using dual fluoroscopy, but differences across segments were difficult to assess because limited segments (L2-L5) were evaluated (Hashemirad et al., 2013; Li et al., 2009; Mellor et al., 2014). Several groups have also evaluated lateral bending and axial rotation in the context of studying coupled movements in lumbar vertebral segments (Fujii et al., 2007; Pearcy et al., 1984; Pearcy and Tibrewal, 1984; Shin et al., 2013). Classically the coupled motions have been described by lumbar vertebral segment rotation around the axial or coronal axis, coupled with out of plane motions along the non-primary axes of rotation in the opposite direction (Panjabi and White III, 1990); the prior studies of standing rotation and lateral bending have reported that this pattern may vary based on segment (Pearcy and Tibrewal, 1984; Shin et al., 2013). We observed when subjects rotated to the left, intervertebral segments displayed movement towards the right in the coronal plane and vice versa. The coupled bending motions were less clear with lateral bending positions, likely due to variability in lateral bending position across subjects. Differences between the prior studies and the current study may also reflect



**Fig. 4.** Local lumbar spine intervertebral angles for sagittal (A; standing, sitting flexion, prone on elbows, prone extension), coronal (B; standing, standing left lateral bending, standing right lateral bending), and axial positions (C; standing, sitting left axial rotation, sitting right axial rotation). Intervertebral angles from L1-L2 (left) to L5-S1 (right) are shown for the primary plane. Statistically significant difference between measurements ( $p < .05$ ) indicated by line. Sit F. = Sitting forward flexion. P.O.E. = Prone on elbows. P. Ext. = Prone extension with elbows extended. Stand L. Bend = Standing left lateral bend. Stand R. Bend = Standing right lateral bend. Sit R. Rot. = Sitting right axial rotation. Sit L. Rot. = Sitting left axial rotation.



**Fig. 5.** Global measure of coronal Cobb angle for coronal positions (standing, standing left lateral bending, standing right lateral bending). Statistically significant difference between measurements ( $p < .05$ ) indicated by line. Stand L. Bend = Standing left lateral bend. Stand R. Bend = Standing right lateral bend.

sex differences in coupling patterns, since the prior studies included mostly male subjects (94% male across both studies), while the current study has greater female representation (60% females).

Previous investigators have evaluated LS IVD characteristics with early-range position changes in supine (Beattie et al., 1994; Brault et al., 1997; Edmondston et al., 2000; Fazey et al., 2006; Fazey et al., 2013; Fazey et al., 2010; Willén et al., 1997), between unloaded and loaded positions, or among early-range loaded sagittal plane positions in both healthy subjects (Alexander et al., 2007; Nazari et al., 2012, 2015; Schmid et al., 1999) and subjects with pathology (Gilbert et al., 2010; Hayashi et al., 2015; Lee et al., 2009; Tarantino et al., 2013; Zou et al., 2009). Consistent with previous findings in early ranges of flexion and extension, we observed posterior migration with end-range flexion and anterior migration with end-range extension (Beattie et al., 1994; Brault et al., 1997; Edmondston et al., 2000; Fennell et al., 1996). These similarities suggest that IVD behavior is similar throughout the range of motion and under different loading conditions in healthy subjects. However, in subjects with disc pathology, IVD behavior appears to be inconsistent (Lee et al., 2009; Zou et al., 2009).

Interestingly, we also observed that IVD height increased posteriorly but did not change anteriorly with end-range flexion, and increased anteriorly, but did not change posteriorly with end-range extension. This, along with a concurrent decrease in A/P IVD length, suggests IVD height changes were not only a function of intervertebral angle, but distraction of the IVD in end-range positions. Additionally, with the POE and PExt positions, the position of the nucleus appears to be more posterior in the upper lumbar spine, and more anterior in the lower lumbar spine. This difference parallels and may be a result of less extension movement in the upper lumbar segments and greater extension movement in the lower lumbar segments. These findings are unique to the current study because kinematics and disc behavior has not been previously reported in these end-range positions.

There are several limitations to this study. Because a limited number of relatively young subjects were tested, the findings from this study may not be generalizable to older adults. Only end-range positions were measured; people with LBP or LS pathology may not be able to hold an end-range position for the duration of an MRI scan. The width of the upright MRI scanner is 48.3 cm, which can curtail the motion of a subject to a single direction and limits the size of subjects that can fit in the scanner. Sitting flexion and rotation positions were selected rather than standing positions in order

to stabilize the pelvis, achieve maximum LS positions, and so that patients were stable for the duration of a scan to avoid motion artifact. Third, based on prior studies, IVD characteristics appear to be different between pathologic and healthy IVDs in early-range sagittal positions (Lee et al., 2009; Zou et al., 2009); however, this would be difficult to evaluate using methods described in the current study, as NP signal decreases with IVD degeneration (Pfirrmann et al., 2001). Also, due to imaging constraints, we were unable to measure NP migration in the coronal or axial planes.

This study investigated changes in LS alignment and IVD characteristics in end-range positions in each cardinal plane of motion in healthy subjects using upright MRI. For sagittal plane positions, the upper lumbar vertebral segments had less mobility than lower segments, but L5-S1 maintained lordosis even with end-range flexion. The NP displayed anterior migration with extension and posterior migration with flexion. In lateral bending, the upper lumbar segments displayed greater mobility than lower segments. With trunk rotation, there was minimal rotation at each intervertebral segment that was coupled with contralateral coronal plane motion. These results provide the framework to help clinicians and researchers better understand LS alignment and IVD characteristics with end-range positions in healthy subjects and can be used to develop more specific biomechanical models and a basis for comparison of people with pathology.

#### Conflict of interest statement


The authors report no conflicts of interest.

#### Acknowledgements

This study was funded by the San Diego State University Grants Program. The study sponsor provided funding, but had no role in the study design, data collection, analysis, interpretation, writing of the manuscript, or decision to submit for publication.


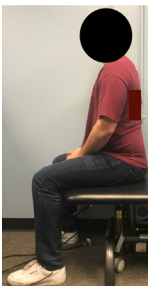



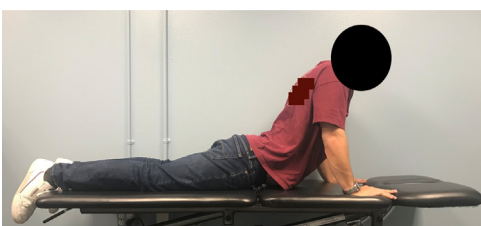
#### Appendix A. Upright MRI testing, positions and instruction set

**General instructions:** “For all positions we will take a short scan to be sure we are focusing on the correct area of the spine. Then we will ask you to hold your position for approximately 2–3 min while we complete the full scan. Please try to breathe in a shallow way, through your chest rather than your stomach to avoid moving the coil that is helping us to get the image.”

Position	Instruction	Figures
Standing	“Please stand comfortably, with your arms at your sides. Be as still as you can and hold your position for approximately 3 min.”	

(continued on next page)

(continued)

Position	Instruction	Figures
<p><b>Standing Lateral Bend (R/L)</b>                      The subject is oriented in parallel with scanner, and a bar is provided for hand support after the patient has moved into position</p>	<p><i>“Keeping your feet in place (comfortable distance apart), please bend to the (right/left) side as far as you possibly can. When you have gone as far as you can, then hold your position while we take the 3-minute scan. Please place your hand on the bar to help stabilize yourself.”</i></p>	
<p><b>Sitting</b>                      The subject is sitting on a wooden stool with his/her back unsupported, a footrest placed at 19" from the seat surface (“standard” seat height), and hands resting in lap</p>	<p><i>“Please sit comfortably, with your arms resting in your lap. Be as still as you can and hold your position while we take the 3-minute scan.”</i></p>	
<p><b>Sitting forward flexion</b>                      From sitting position above</p>	<p><i>“Keeping you buttocks on the seat, please bend forward as far as you can, like you are trying to touch your toes. When you have gone as far as you can, then hold your position, while we take the 3-minute scan.”</i></p>	
<p><b>Sitting rotation</b>                      From sitting position above, with elbows bent and palms resting on chest/shoulders/clavicle area, and a bar in front of subject at elbow level for support</p>	<p><i>Keeping you buttocks on the seat, please rotate your trunk to the (right/left) side as far as you possibly can. When you have gone as far as you can, then hold your position while we take the 3-minute scan. You can use your hand on the bar to stabilize yourself, but don't use it to push you further into rotation.”</i></p>	
<p><b>Prone on elbows</b>                      The subject is prone on the MRI table, with forearms and palms on the surface of the table and upper arms vertical, supporting the trunk in slight extension</p>	<p><i>“Please prop yourself up on your elbows and forearms with your palms on the table (like sphinx or cobra pose in yoga, demonstrate). Be as still as you can and hold your position, while we take the 3-minute scan.”</i></p>	
<p><b>Prone extension</b>                      From prone position above</p>	<p><i>“Please push into your hands to straighten your arms and push your trunk up off the table, but keeping your pelvis on/near the table (like upward dog in yoga, demonstrate). When you have gone as far as you can, then hold your position while we take the 3-minute scan.”</i></p>	



## Appendix B. Supplementary material

Supplementary data to this article can be found online at <https://doi.org/10.1016/j.jbiomech.2019.04.020>.

## References

- Alexander, L.A., Hancock, E., Agouris, I., Smith, F.W., MacSween, A., 2007. The response of the nucleus pulposus of the lumbar intervertebral discs to functionally loaded positions. *Spine* 32, 1508–1512.
- Alyas, F., Sutcliffe, J., Connell, D., Saifuddin, A., 2010. Morphological change and development of high-intensity zones in the lumbar spine from neutral to extension positioning during upright MRI. *Clin. Radiol.* 65, 176–180.
- Andersson, G.B., 1999. Epidemiological features of chronic low-back pain. *Lancet* 354, 581–585.
- Beattie, P.F., Brooks, W.M., Rothstein, J.M., Sibbitt, J.W., Robergs, R.A., MacLean, T., Hart, B.L., 1994. Effect of lordosis on the position of the nucleus pulposus in supine subjects. A study using magnetic resonance imaging. *Spine* 19, 2096–2102.
- Berry, D.B., Rodríguez-Soto, A.E., Tokunaga, J.R., Gombatto, S.P., Ward, S.R., 2015. An endplate-based joint coordinate system for measuring kinematics in normal and abnormally-shaped lumbar vertebrae. *J. Appl. Biomech.* 31, 499–503.
- Berry, D.B., Rodríguez-Soto, A.E., Su, J., Gombatto, S.P., Shahidi, B., Palombo, L., Chung, C., Jensen, A., Kelly, K.R., Ward, S.R., 2017. Lumbar spine postures in Marines during simulated operational positions. *J. Orthop. Res.* 35, 2145–2153.
- Brault, J.S., Driscoll, D.M., Laakso, L.L., Kappler, R.E., Allin, E.F., Glonek, T., 1997. Quantification of lumbar intradiscal deformation during flexion and extension, by mathematical analysis of magnetic resonance imaging pixel intensity profiles. *Spine* 22, 2066–2072.
- Choi, K.-C., Kim, J.-S., Jung, B., Lee, S.-H., 2009. Dynamic lumbar spinal stenosis: the usefulness of axial loaded MRI in preoperative evaluation. *J. Korean Neurosurg. Soc.* 46, 265–268.
- Cobb, J.R., 1948. Outline for the study of scoliosis. *Instr. Course Lect.*
- Edmondston, S., Song, S., Bricknell, R., Davies, P., Fersum, K., Humphries, P., Wickenden, D., Singer, K., 2000. MRI evaluation of lumbar spine flexion and extension in asymptomatic individuals. *Manual Therapy* 5, 158–164.
- Fazey, P.J., Song, S., Mønsås, Å., Johansson, L., Haukalid, T., Price, R.I., Singer, K.P., 2006. An MRI investigation of intervertebral disc deformation in response to torsion. *Clin. Biomech.* 21, 538–542.
- Fazey, P.J., Song, S., Price, R.I., Singer, K.P., 2013. Nucleus pulposus deformation in response to rotation at L1–2 and L4–5. *Clin. Biomech.* 28, 586–589.
- Fazey, P.J., Takasaki, H., Singer, K.P., 2010. Nucleus pulposus deformation in response to lumbar spine lateral flexion: an in vivo MRI investigation. *Eur. Spine J.* 19, 1115–1120.
- Fennell, A.J., Jones, A.P., Hukins, D.W., 1996. Migration of the nucleus pulposus within the intervertebral disc during flexion and extension of the spine. *Spine* 21, 2753–2757.
- Fujii, R., Sakaura, H., Mukai, Y., Hosono, N., Ishii, T., Iwasaki, M., Yoshikawa, H., Sugamoto, K., 2007. Kinematics of the lumbar spine in trunk rotation: in vivo three-dimensional analysis using magnetic resonance imaging. *Eur. Spine J.* 16, 1867–1874.
- Gilbert, J.W., Martin, J.C., Wheeler, G.R., Storey, B.B., Mick, G.E., Richardson, G.B., Herder, S.L., Gyarteng-Dakwa, K., Broughton, P.G., 2010. Lumbar disk protrusion rates of symptomatic patients using magnetic resonance imaging. *J. Manipulative Physiol. Ther.* 33, 626–629.
- Gombatto, S.P., Collins, D.R., Sahrman, S.A., Engsborg, J.R., Van Dillen, L.R., 2007. Patterns of lumbar region movement during trunk lateral bending in 2 subgroups of people with low back pain. *Phys. Ther.* 87, 441–454.
- Gunzburg, R., Hutton, W., Fraser, R., 1991. Axial rotation of the lumbar spine and the effect of flexion: an in vitro and in vivo biomechanical study. *Spine* 16, 22–28.
- Hashemirad, F., Hatf, B., Jaberzadeh, S., Agha, N.A., 2013. Validity and reliability of skin markers for measurement of intersegmental mobility at L2–3 and L3–4 during lateral bending in healthy individuals: a fluoroscopy study. *J. Bodywork Move. Therapies* 17, 46–52.
- Hayashi, T., Daubs, M.D., Suzuki, A., Scott, T.P., Phan, K.H., Ruangchainikom, M., Takahashi, S., Shiba, K., Wang, J.C., 2015. Motion characteristics and related factors of Modic changes in the lumbar spine. *J. Neurosurg.: Spine* 22, 511–517.
- Hedberg, K., Alexander, L.A., Cooper, K., Hancock, E., Ross, J., Smith, F.W., 2013. Low back pain: an assessment using positional MRI and MDT. *Manual Therapy* 18, 169–171.
- Karadimas, E.J., Siddiqui, M., Smith, F.W., Wardlaw, D., 2006. Positional MRI changes in supine versus sitting postures in patients with degenerative lumbar spine. *Clin. Spine Surg.* 19, 495–500.
- Keorochana, G., Taghavi, C.E., Lee, K.-B., Yoo, J.H., Liao, J.-C., Fei, Z., Wang, J.C., 2011. Effect of sagittal alignment on kinematic changes and degree of disc degeneration in the lumbar spine: an analysis using positional MRI. *Spine* 36, 893–898.
- Kettler, A., Marin, F., Sattelmayer, G., Mohr, M., Mannel, H., Dürsel, L., Claes, L., Wilke, H., 2004. Finite helical axes of motion are a useful tool to describe the three-dimensional in vitro kinematics of the intact, injured and stabilised spine. *Eur. Spine J.* 13, 553–559.
- Kong, M.H., Morishita, Y., He, W., Miyazaki, M., Zhang, H., Wu, G., Hymanson, H.J., Wang, J.C., 2009. Lumbar segmental mobility according to the grade of the disc, the facet joint, the muscle, and the ligament pathology by using kinetic magnetic resonance imaging. *Spine* 34, 2537–2544.
- Kulig, K., Powers, C.M., Landel, R.F., Chen, H., Fredericson, M., Guillet, M., Butts, K., 2007. Segmental lumbar mobility in individuals with low back pain: in vivo assessment during manual and self-imposed motion using dynamic MRI. *BMC Musculoskeletal Disorders* 8, 8.
- Lao, L., Daubs, M.D., Scott, T.P., Lord, E.L., Cohen, J.R., Yin, R., Zhong, G., Wang, J.C., 2015. Effect of disc degeneration on lumbar segmental mobility analyzed by kinetic magnetic resonance imaging. *Spine* 40, 316–322.
- Lee, C.S., Hwang, C.J., Lee, S.-W., Ahn, Y.-J., Kim, Y.-T., Lee, D.-H., Lee, M.Y., 2009. Risk factors for adjacent segment disease after lumbar fusion. *Eur. Spine J.* 18, 1637.
- Li, G., Wang, S., Passias, P., Xia, Q., Li, G., Wood, K., 2009. Segmental in vivo vertebral motion during functional human lumbar spine activities. *Eur. Spine J.* 18, 1013–1021.
- MacWilliams, B.A., Rozumalski, A., Swanson, A.N., Werve, R., Dykes, D.C., Novacheck, T.F., Schwartz, M.H., 2014. Three-dimensional lumbar spine vertebral motion during running using indwelling bone pins. *Spine* 39, E1560–E1565.
- Madsen, R., Jensen, T.S., Pope, M., Sørensen, J.S., Bendix, T., 2008. The effect of body position and axial load on spinal canal morphology: an MRI study of central spinal stenosis. *Spine* 33, 61–67.
- Mellor, F.E., Thomas, P.W., Thompson, P., Breen, A.C., 2014. Proportional lumbar spine inter-vertebral motion patterns: a comparison of patients with chronic, non-specific low back pain and healthy controls. *Eur. Spine J.* 23, 2059–2067.
- Nazari, J., Pope, M.H., Graveling, R.A., 2012. Reality about migration of the nucleus pulposus within the intervertebral disc with changing postures. *Clin. Biomech.* 27, 213–217.
- Nazari, J., Pope, M.H., Graveling, R.A., 2015. Feasibility of Magnetic resonance imaging (MRI) in obtaining nucleus pulposus (NP) water content with changing postures. *Magn. Reson. Imaging* 33, 459–464.
- Neuschwander, T.B., Cutrone, J., Macias, B.R., Cutrone, S., Murthy, G., Chambers, H., Hargens, A.R., 2010. The effect of backpacks on the lumbar spine in children: a standing magnetic resonance imaging study. *Spine* 35, 83–88.
- Nguyen, H.S., Doan, N., Shabani, S., Baisden, J., Wolfla, C., Paskoff, G., Shender, B., Stemper, B., 2016. Upright magnetic resonance imaging of the lumbar spine: Back pain and radiculopathy. *J. Craniover. Junction Spine* 7, 31.
- Panjabi, M.M., Takata, K., Goel, V.K., 1983. Kinematics of lumbar intervertebral foramen. *Spine* 8, 348–357.
- Panjabi, M.M., White III, A.A., 1990. Basic biomechanics of the spine. *Neurosurgery* 7, 76–93.
- Passias, P.G., Wang, S., Kozanek, M., Xia, Q., Li, W., Grottkau, B., Wood, K.B., Li, G., 2011. Segmental lumbar rotation in patients with discogenic low back pain during functional weight-bearing activities. *J. Bone Joint Surg. Am. Vol.* 93, 29.
- Pearcy, M., Portek, I., Shepherd, J., 1984. Three-dimensional x-ray analysis of normal movement in the lumbar spine. *Spine* 9, 294–297.
- Pearcy, M., Tibrewal, S., 1984. Axial rotation and lateral bending in the normal lumbar spine measured by three-dimensional radiography. *Spine* 9, 582–587.
- Pfirmsmann, C.W., Metzendorf, A., Zanetti, M., Hodler, J., Boos, N., 2001. Magnetic resonance classification of lumbar intervertebral disc degeneration. *Spine* 26, 1873–1878.
- Rodríguez-Soto, A.E., Berry, D.B., Jaworski, R., Jensen, A., Chung, C.B., Niederberger, B., Qadir, A., Kelly, K.R., Ward, S.R., 2016a. The effect of training on lumbar spine posture and intervertebral disc degeneration in active-duty Marines. *Ergonomics*, 1–9.
- Rodríguez-Soto, A.E., Berry, D.B., Palombo, L., Valaik, E., Kelly, K.R., Ward, S.R., 2016b. The effect of load magnitude and distribution on lumbar spine posture in active-duty marines. *Spine* 42, 345–351.
- Rodríguez-Soto, A.E., Jaworski, R., Jensen, A., Niederberger, B., Hargens, A.R., Frank, L. R., Kelly, K.R., Ward, S.R., 2013. Effect of load carriage on lumbar spine kinematics. *Spine (Phila Pa 1976)* 38, E783–791.
- Rosset, A., Spadola, L., Ratib, O., 2004. OsiriX: an open-source software for navigating in multidimensional DICOM images. *J. Digit. Imaging* 17, 205–216.
- Saifuddin, A., Blease, S., MacSweeney, E., 2003. Axial loaded MRI of the lumbar spine. *Clin. Radiol.* 58, 661–671.
- Schmid, M.R., Stucki, G., Duestel, S., Wildermuth, S., Romanowski, B., Hodler, J., 1999. Changes in cross-sectional measurements of the spinal canal and intervertebral foramina as a function of body position: in vivo studies on an open-configuration MR system. *AJR Am. J. Roentgenol.* 172, 1095–1102.
- Scholtes, S.A., Gombatto, S.P., Van Dillen, L.R., 2009. Differences in lumbopelvic motion between people with and people without low back pain during two lower limb movement tests. *Clin. Biomech.* 24, 7–12.
- Shin, J.-H., Wang, S., Yao, Q., Wood, K.B., Li, G., 2013. Investigation of coupled bending of the lumbar spine during dynamic axial rotation of the body. *Eur. Spine J.* 22, 2671–2677.
- Shymon, S., Hargens, A.R., Minkoff, L.A., Chang, D.G., 2014a. Body posture and backpack loading: an upright magnetic resonance imaging study of the adult lumbar spine. *Eur. Spine J.* 23, 1407–1413.
- Shymon, S.J., Yaszay, B., Dwek, J.R., Proudfoot, J.A., Donohue, M., Hargens, A.R., 2014b. Altered disc compression in children with idiopathic low back pain: an upright MRI backpack study. *Spine* 39, 243.
- Simonetti, G., Masala, S., 2003. Axial loading MRI of the lumbar spine. *In vivo* 17, 413–420.
- Tarantino, U., Fanucci, E., Iundisi, R., Celi, M., Altobelli, S., Gasbarra, E., Simonetti, G., Manenti, G., 2013. Lumbar spine MRI in upright position for diagnosing acute and chronic low back pain: statistical analysis of morphological changes. *J. Orthopaedics Traumatol.* 14, 15–22.

- Wang, S., Passias, P., Li, G., Li, G., Wood, K., 2008. Measurement of vertebral kinematics using noninvasive image matching method—validation and application. *Spine* 33, E355–E361.
- Willén, J., Danielson, B., Gaulitz, A., Niklason, T., Schönström, N., Hansson, T., 1997. Dynamic effects on the lumbar spinal canal: axially loaded CT-myelography and MRI in patients with sciatica and/or neurogenic claudication. *Spine* 22, 2968–2976.
- Wu, M., Wang, S., Driscoll, S.J., Cha, T.D., Wood, K.B., Li, G., 2014. Dynamic motion characteristics of the lower lumbar spine: implication to lumbar pathology and surgical treatment. *Eur. Spine J.* 23, 2350–2358.
- Yang, Z., Ma, H.T., Wang, D., Lee, R., 2008. Year Error analysis on spinal motion measurement using skin mounted sensors. In *Engineering in Medicine and Biology Society, 2008. EMBS 2008. 30th Annual International Conference of the IEEE*.
- Zou, J., Yang, H., Miyazaki, M., Morishita, Y., Wei, F., McGovern, S., Wang, J.C., 2009. Dynamic bulging of intervertebral discs in the degenerative lumbar spine. *Spine* 34, 2545–2550.